# Evaluation of solution methods for radiative heat transfer in gaseous oxy-fuel combustion environments

Porter, R.; Liu, F.; Pourkashanian, M.; Williams, A.; Smith, D.



**Publisher's version / Version de l'éditeur:**
https://doi.org/10.1016/j.jqsrt.2010.04.028
*Journal of Quantitative Spectroscopy and Radiative Transfer, 111, 14, pp. 2084-2094, 2010-05-01*

Journal of Quantitative Spectroscopy & Radiative Transfer 111 (2010) 2084–2094

Contents lists available at ScienceDirect

Journal of Quantitative Spectroscopy & Radiative Transfer

journal homepage: www.elsevier.com/locate/jqsrt

# Evaluation of solution methods for radiative heat transfer in gaseous oxy-fuel combustion environments

R. Porter [a,*], F. Liu [b], M. Pourkashanian [a], A. Williams [a], D. Smith [c]

[a] Centre for Computational Fluid Dynamics, University of Leeds, Leeds, LS2 9JT, UK
[b] National Research Council Canada, Ottawa, Ontario, Canada K1A 0R6
[c] Doosan Babcock Energy Limited, Porterfield Road, Renfrew, PA4 8DJ, UK

ARTICLE INFO

*Article history:*
Received 17 December 2009
Received in revised form
23 April 2010
Accepted 27 April 2010

*Keywords:*
Radiative transfer
Non-gray gas models
Full spectrum *k*-distribution
Discrete ordinates method
Oxy-fuel combustion
Computational fluid dynamics

ABSTRACT

The exact solution to radiative heat transfer in combusting flows is not possible analytically due to the complex nature of the integro-differential radiative transfer equation (RTE). Many different approximate solution methods for the solution of the RTE in multi-dimensional problems are available. In this paper, two of the principal methods, the spherical harmonics ($P_1$) and the discrete ordinates method (DOM) are used to calculate radiation. The radiative properties of the gases are calculated using a non-gray gas full spectrum *k*-distribution method and a gray method. Analysis of the effects of numerical quadrature in the DOM and its effect on computation time is performed. Results of different radiative property methods are compared with benchmark statistical narrow band (SNB) data for both cases that simulate air combustion and oxy-fuel combustion. For both cases, results of the non-gray full spectrum *k*-distribution method are in good agreement with the SNB data. In the case of oxy-fuel simulations with high partial pressures of carbon dioxide, use of gray method for the radiative properties may cause errors and should be avoided.



## 1. Introduction

In modelling combustion, the accurate calculation of heat transfer by radiation is essential to ensure good predictions for the flame temperature and also because of coupling with chemical reactions, turbulence and pollutant prediction. Incorrect prediction of the radiation and temperature fields can have a detrimental effect on the prediction of combustion products and emission of trace species. In the combustion of hydrocarbon fuels, the major products i.e. carbon dioxide ($CO_2$) and water vapour ($H_2O$) interact with radiation by absorption and emission. These gases have strong absorption bands in the spectrum at temperatures relevant to combustion due to ro–vibrational transitions. Often in computational fluid dynamics (CFD) calculations of combustion and radiation, the gases are assumed to be gray hence there is no spectral dependence on the absorption or emission. This is essentially done to reduce the computation time to solve the radiative transfer equation (RTE). Oxy-fuel combustion is a new technology under development as one of the portfolio of options for reducing greenhouse gas emissions by carbon capture and storage (CCS). In oxy-fuel combustion with recycled flue gas [1], nitrogen ($N_2$) is separated from air and fuel is burnt in pure oxygen with the remainder of the oxidiser composed of recycled flue gases (RFG). This technology produces a flue gas stream that has very high concentrations of $CO_2$ and thus makes CCS more economical with a lower efficiency penalty. In an oxy-fuel combustion environment, the non-gray nature of the combustion gases becomes even more important because of the increased partial pressures. It is, therefore, essential to use a non-gray model to correctly predict the

* Corresponding author. Tel.: +44 113 343 481; fax: +44 113 246 7310.
*E-mail address:* pmrp@leeds.ac.uk (R. Porter).

0022-4073/$ - see front matter © 2010 Elsevier Ltd. All rights reserved.
doi:10.1016/j.jqsrt.2010.04.028

absorption and emission within the furnace environment. In CFD combustion calculations, the main consideration apart from accuracy is the computation time and this can be one of the deciding factors when assessing which combination of RTE solution method and radiative property model to use.

## 2. Solution methods for RTE

The RTE, Eq. (1), describes the transport of radiative intensity through a medium.

$$\frac{dI_\lambda(\vec{r},\vec{s})}{ds} = -(\kappa_{a,\lambda}+\sigma_{s\lambda})I_\lambda(\vec{r},\vec{s}) + \kappa_{a,\lambda}I_{\lambda,b} + \frac{\sigma_{s\lambda}}{4\pi}\int_{\Omega=0}^{4\pi} I'_\lambda(\vec{r},\vec{s})'\Phi(\vec{s}\cdot\vec{s}')d\Omega' \quad (1)$$

The intensity $I_\lambda(\vec{r},\vec{s})$ at a particular wavelength $\lambda$, position $\vec{r}$ in direction $\vec{s}$ is attenuated by absorption and scattering as it travels and is augmented by in-scattering and emission from the medium. The properties of the medium, the absorption coefficient, $\kappa_{a,\lambda}$, and scattering coefficient, $\sigma_{s\lambda}$, determine the amount of attenuation and are dependent upon the wavelength. $\Phi(\vec{s}\cdot\vec{s}')$ is the scattering phase function that provides the directional dependence of the scattering. The RTE is a complex integro-differential equation that is very time consuming to solve even for a simple 1-D case and therefore an exact analytical solution to the equation is in general not possible [2]. The boundary conditions of the RTE are given in Eq. (2) with $\rho_\lambda$ the reflectivity of the wall, and assuming that the wall is opaque, gray and diffusely reflecting

$$I_\lambda(\vec{r}_w,\vec{s}) = \varepsilon_w I_b(\vec{r}_w) + \frac{\rho_\lambda}{\pi}\int_{\vec{n}\cdot\vec{s}'<0} I'_\lambda(\vec{s}')|\vec{n}\cdot\vec{s}'|d\Omega' \quad (2)$$

Several robust methods have been developed to approximate the solution of the RTE, including the spherical harmonics ($P_1$) method [3,4], the discrete ordinates method (DOM) [5,6] and the discrete transfer ray-tracing method (DTRM) [7]. In commercial CFD codes the methods of solution that are widely available are the $P_1$, DOM and DTRM. However, in the commercial software employed here the DTRM is only applicable for cases with a non-scattering medium and therefore not suitable for coal combustion environments. This is because the particulates in coal combustion including char and ash may be highly scattering, affecting the calculated attenuation of radiation. Hence to obtain the most accurate solution, the scattering should not be neglected.

The $P_1$ method is a spherical harmonics method. The radiation intensity can be expanded into a series of spherical harmonics, and the $P_1$ method is the sequence truncated after the first term, $P_3$ is the series truncated after the third term and so on. The accuracy normally required in CFD radiative modelling yields the $P_1$ method suitable, especially when the increased computation times for higher order methods are taken into consideration. The $P_1$ method permits the total radiative intensity over all solid angles, $G$, to be written as a Helmholtz equation, Eq. (4) [8].

$$G = \int_{4\pi} I\,d\Omega \quad (3)$$

$$\nabla\left(\frac{1}{3(\kappa_a+\sigma_s)}\nabla G\right) - \kappa_a G + 4\kappa_a\sigma T^4 = 0 \quad (4)$$

This enables the incident radiation to be solved as a scalar quantity within CFD codes. However the drawback of this method is obvious because only the total incident radiation is solved under the assumption that the radiation intensity depends linearly on the direction cosines and therefore is less accurate in situations where the radiation intensity exhibits strong angular dependence. In Eqs. (3–5), the dependence on wavenumber has been omitted, so that a gray approximation is shown. The boundary conditions are given by Eq. (5).

$$-\frac{2}{3}\hat{n}\cdot\nabla G + \kappa_a G = 4\pi\kappa_a I_b \quad (5)$$

The DOM utilizes a different approach for solving the RTE. The solid angle is split up into a number of discrete directions and the radiative intensity is assumed to be constant within each division of the solid angle. The RTE must be solved for the number of discrete angles that are specified, with weights associated with each discrete direction. The method is more time consuming than the $P_1$ method because the solution is required for many different directions. In a 3-D case (gray formulation) the RTE has the form of Eq. (6) [5].

$$\mu_m\frac{\partial I^m}{\partial x} + \eta_m\frac{\partial I^m}{\partial y} + \xi_m\frac{\partial I^m}{\partial z} = -\kappa_a I^m + \kappa_a I_b + \frac{\sigma_s}{4\pi}\sum_{m'}^{N} I^m\Phi^{m'm}w^m \quad (6)$$

In Eq. (6), $\mu_m$,$\eta_m$ and $\xi_m$ are the direction cosines, superscript $m$ denotes the $m$th angle in the quadrature and $w^m$ the weights for the angular discretization. A finite difference form of the equation, Eq. (7) is used to solve for the intensity at cell centres (non-scattering).

$$\mu_m A(I^m_{xe}-I^m_{xr}) + \eta_m B(I^m_{ye}-I^m_{yr}) + \xi_m C(I^m_{ze}-I^m_{zr}) = -\kappa_a V_p I^m_p + \kappa_a V_p I_b \quad (7)$$

where $I^m_{xe}$,$I^m_{xr}$,$I^m_{ye}$,$I^m_{yr}$,$I^m_{ze}$,$I^m_{zr}$ are the intensities at the faces of the control volume, $I^m_p$ the intensity at the centre of the cell, $A$,$B$,$C$ the areas of the faces of the control volume and $V_p$ the total volume of the control volume. The cell centre value for the intensity is determined from the values at the cell faces, commonly using a diamond or step spatial discretization scheme.

In general, the Monte Carlo method may produce the most accurate solution of the RTE because it is based on a large number of simulated rays with errors coming only from statistical noise [2]. However, it requires a large number of simulated rays and very long computation times to give an accurate solution. Hence when coupled with CFD there are issues with computation time and also with compatibility of CFD grids with Monte Carlo calculations. For many combustion cases, the DOM is often the more accurate solution to the RTE for several reasons. Firstly it is valid for a wide range of optical thicknesses, whereas the $P_1$ method, since it lacks

adequate directionality, inherently assumes that the radiation is weakly dependent on direction. This assumption implies that the $P_1$ method is reasonably accurate in optically thick media and therefore the method may produce erroneous results if used when the optical thickness is low [4]. However, the best method to use is dependent upon the case in question. The accuracy of the results obtained by the DOM is dependent upon the geometrical shape, the overall optical dimension of the problem and the level of quadrature that is employed. The most common quadrature used is the $S_2$ quadrature, as a compromise for accuracy and efficiency. Increasing the level of quadrature for the DOM significantly increases the computation time.

Unfortunately due to the complex nature of the RTE, many of the popular solution methods suffer from inaccuracies. In the spherical harmonics method, errors are introduced into the solution when the optical thickness is low and the boundary conditions at the walls are subject to various interpretations [9]. The DOM suffers from ray effects and (in CFD implementation) false scattering. These errors are introduced by the angular and spatial discretization. Ray effects can be reduced by increasing the quadrature divisions, however the computation time is compromised. Also the false scattering and ray effects are not uniquely independent and increasing the angular quadrature may increase false scattering whilst decreasing observed ray effects [10]. The DTRM has inaccuracies due to lack of scattering in the medium, also if a case with particles is considered then due to the pre-processor ray-tracing, the absorption and scattering by the particles is neglected. In the case of coal combustion this could be very important because radiation is a key mechanism in raising particles surface temperature and predicting the particle ignition delay time. Additionally the particles surface temperatures whilst undergoing combustion are observed from experiments to be 200–300 K hotter than the surrounding gases and possibly even higher than this depending upon combustion conditions, including particle size and oxygen concentration [11,12]. Hence this means that they may have a significant impact on heat transfer in the flame region. Disregarding the particle interaction with radiation could limit calculation accuracy of a combustion simulation in coal combustion cases.

The link between radiation and temperature calculation in CFD is by the (gray) radiation source term in the energy equation, Eq. (8).

$$\nabla q = \kappa_a \left( 4\pi I_b - \int_{4\pi} I \, \mathrm{d}\boldsymbol{\Omega} \right) \tag{8}$$

## 3. Radiative properties of gases

Radiative property models can broadly be grouped into three categories; line-by-line methods, band models and global methods. Line-by-line (LBL) methods are based directly on spectroscopic databases and are the most accurate method for calculating the radiative property of gases. The LBL method is flexible because it can be used over all spectral values from microwave to ultra-violet and hence can be used for many applications. However the very long computation time required to solve potentially millions of RTE equations required at high temperatures causes this method to be prohibited for combustion calculations. Band models include popular models such as Goody's statistical narrow band model (SNB) [13] and Edwards exponential wide band model (EWBM) [14] and more recently developments such as the statistical narrow-band correlated-$k$ (SNBCK) [15] and narrow band $k$-distribution methods [16]. While several of these models can provide very accurate results when compared to LBL methods, they are generally also too time consuming for engineering applications, and are more often used to generate benchmark data. Modifications have been made for several of these methods to reduce the computation time without significantly losing accuracy [17,18]. When considering the applicability of methods to combustion cases, it should be considered that for traditional formulations of band models theoretically require that scattering is neglected and as discussed earlier, this may reduce the accuracy of the simulation.

Global methods have the lowest computation time of all the methods and thus are often the preferred choice if non-gray gas modelling is undertaken in CFD. There are several methods that are well established and provide accurate results for modelling the properties of major combustion products such as $CO_2$ and $H_2O$, including the spectral line-based weighted sum of gray-gases method (SLW) [19,20], the full-spectrum $k$-distribution method (FSK) [8,16,21] and the absorption distribution function method (ADF) [22]. A recent paper explains in detail the relationship between these three methods [23].

The FSK method has been derived from an approach based on narrow band $k$-distributions. The method works by re-ordering the dependence of the absorption coefficient on wavenumber. Over a narrow band in the spectrum it is observed that the absorption coefficient of a gas may vary erratically (depending on the temperature and pressure) but other properties dependent on the wavenumber such as the Planck function are essentially constant [8]. The same absorption coefficient may be observed at several different wavenumbers over the narrow band and thus the distribution can be re-ordered into a 'probability density function', or $k$-distribution of absorption coefficient ($f(k)$). The $f(k)$ distribution reduces the number of calculations and helps to smoothen the erratic variation. The $f(k)$ distribution is applicable only for homogenous and isothermal media, and $k$ is unbounded which produces difficulties when using numerical quadrature. A cumulative $f(k)$ distribution can be constructed, $g(k)$, Eq. (9), which is bound between 0 and 1 and is also suitable for inhomogeneous or non-isothermal media, thus making it a more attractive option.

$$g(\overline{\phi}_0,k) = \int_0^k f(\overline{\phi}_0,k)\mathrm{d}k \tag{9}$$

The resulting function is smooth and monotonically increasing between the limits 0 and 1. $\overline{\phi} = (T,p,\overline{\mathrm{x}})$ is the vector containing the local values of temperature,

pressure and mole fraction of species.$\overline{\phi}_0$ is this vector at the reference state $\overline{\phi}_0=(T_0,p_0,\overline{x}_0)$. To calculate the total intensity over a narrow band, the RTE would ordinarily have to be integrated over wavenumber which is very time consuming. Re-ordering the wavenumber and writing the RTE in terms of $g(k)$ distribution, reduces the number of computations that must be carried out to numerically integrate the function because much lower values of quadrature points can be applied to the cumulative function in order to calculate the intensity over a narrow band.

The same principle can be adopted over the full spectrum but weighting must be used to account for the change in the Planck function over the spectrum. The method has been demonstrated in several papers by Modest and co-workers [16,21,24]. The RTE can be re-written in terms of the $g(k)$ distributions instead of wavenumbers as shown in Eq. (10).

$$\frac{dI_g}{ds}=k^*(T_0,\overline{\phi},g_0)\left[a(T,T_0,g_0)I_b(T)-I_g\right]-\sigma_s\left(I_g-\frac{1}{4\pi}\int_{4\pi}I_g(\hat{s}')\boldsymbol{\Phi}(\hat{s},\hat{s}')d\boldsymbol{\Omega}'\right) \tag{10}$$

with the weighting function between the reference and local state given by Eq. (11).

$$a(T,T_0,g_0)=\frac{f(T,\overline{\phi}_0,k)}{f(T_0,\overline{\phi}_0,k)}=\frac{dg(T,\overline{\phi}_0,k)}{dg_0(T_0,\overline{\phi}_0,k)} \tag{11}$$

It is assumed that scattering is gray in Eq. (10).

Due to the smooth nature of the cumulative function, the number of quadrature points required to integrate over the re-ordered wavenumber is several orders of magnitude less than if the integration over wavenumber was carried out. It has been shown that using ten or fewer quadrature points can be sufficient. The $k$-distributions required in the FSK method can be calculated in two different ways. They can be compiled directly from high accuracy spectroscopic databases such as HITEMP or CDSD-1000, or the full spectrum $k$-distributions can be compiled from narrow band (NB) $k$-distributions. Wang and Modest created a database of pre-compiled NB $k$-distributions and demonstrated only very small loss of accuracy when compared to generation from LBL databases [25]. The benefit to using pre-complied NB $k$-distributions is a reduction in computation time, and so this method is adopted for predicting the radiative properties of the gases in CFD modelling. If a spectroscopic database is used directly to calculate the FSK distributions, then the applicability to the problem at hand must be analysed, for example it must be ensured that the database is accurate at higher temperatures for combustion calculations.

If the gaseous medium under consideration is homogeneous and isothermal, then the FSK distributions are essentially exact, with errors being introduced only from the number and method of quadrature selected and the compilation from NB $k$-distributions. In a combustion environment the partial pressure of combustion gases is non-homogeneous and strong temperature gradients may also be present. Hence approximations must be incorporated into the calculation of the radiative properties to account for the mixing of gases, and the departure from a homogeneous and/or isothermal medium. In particular when considering the calculation of the $k$-distributions either a correlated or scaled assumption must be used. In the scaling approximation, it is assumed that the dependence of the absorption coefficient on wavenumber can be separated from the spatial dependence on concentration, pressure and temperature. Therefore the absorption coefficient can be written as Eq. (12).

$$\kappa_\eta(\eta,\overline{\phi})=k_\eta(\eta)u(\overline{\phi}) \tag{12}$$

The other choice is the correlated assumption. It is assumed that when $\kappa_\eta(\eta,\overline{\phi}_0)$ has a value $k$, then $\kappa_\eta(\eta,\overline{\phi})$ has one unique value $k^*$ i.e. the maximum absorption coefficient in one physical state, will occur at that same wavenumber at a different physical state. The choice of whether to adopt a scaling or correlated approximation depends on the case that is being modelled [16]. In the work presented here the correlated approximation in CFD has been used and from this point forward the method is known as full spectrum correlated $k$-distributions (FSCK). In the work presented 9 quadrature points were used for the numerical calculation of the integration over the spectrum.

The values of temperature, species concentration and pressure chosen for the reference state can have a large impact on the calculated full spectrum $k$-distributions and it is important to select these parameters carefully for the case that is being modelled. The species and pressure may be calculated by a volume-weighted average. For the temperature it is desirable to use a reference value that takes account of the increased emission from high temperatures. Therefore an emission weighted temperature is used

$$T_{avg}=\frac{\int_0^\infty T\kappa_p T_g{}^4\,d\eta}{\int_0^\infty \kappa_p T_g{}^4\,d\eta} \tag{13}$$

## 4. Results and discussion

To assess the accuracy of the FSCK method with different solutions to the RTE in CFD, radiation modelling using the DOM and $P_1$ method has been carried out and compared to benchmark SNB data that has been used as a reference case by several other authors [18,26]. The computation time for the SNB data is far in excess of the FSCK method. The method for solving the RTE for the SNB data is a ray tracing method with $T_7$ quadrature. Errors associated with simulated results have many different origins, one of which may be the difference in the underlying spectral data used. The FSCK distributions are based on HITEMP and CDSD-1000. The SNB data is based on updated band parameters of Soufiani and Taine [27] based on the approximate spectroscopic databases using data from HITRAN 92 with additional lines at high temperatures. The Curtis–Godson approximation is used for non-isothermal and/or non-homogeneous mixtures.

Several cases have been examined, focussing on conditions that have temperatures and species

concentrations relevant to combustion. For all cases examined the pressure is atmospheric.

### 4.1. Case 1 (Air fired concentrations)

The first validation case (Case 1) is presented in a paper by Liu [28]. A box of dimensions 2 m × 2 m × 4 m with black walls at 300 K is modelled. The concentrations of $CO_2$ and $H_2O$ in the medium are prescribed to be 10% and 20% by mole fraction. The temperature profile is prescribed based on the axial and radial co-ordinates. The temperature profile within the enclosure is prescribed in Eqs. (14 and 15).

$$T = (T_c - T_e) f\left(\frac{r}{R}\right) + T_e \tag{14}$$

where $T_c$ is the centreline temperature and $T_e$ the temperature at the end ($z$=4 m).

$$f\left(\frac{r}{R}\right) = 1 - 3\left(\frac{r}{R}\right)^2 + 2\left(\frac{r}{R}\right)^3 \tag{15}$$

where $R$ is the radius of a circle 1 m and $r$ the distance from the enclosure centreline. The centreline temperature varies throughout the enclosure. At $z$=0 m the temperature is 400 K, rising linearly to 1800 K at $z$=0.375 m. The temperature decreases linearly from $z$=0.375 to 4 m, where the temperature is 800 K. The data computed is the net heat flux to the walls of the enclosure and the radiative source terms. It is important to be able to correctly calculate the radiative source term in CFD because this provides the link between the energy equation and the radiation. The prescribed temperature profiles are shown in Fig. 1. The number of grid points used corresponds to the benchmark data by Liu [28], i.e. 17 × 17 × 24 with a greater concentration of nodes in axial direction around the areas of high temperature.

Three different methods of solution to the RTE have been investigated with the FSCK method as the solution for the radiative properties. They are:

1. $P_1$ method
2. DOM with equal numerical quadrature divisions in each octant of solid angle in $\vartheta,\phi$ directions of $N_\vartheta,N_\phi$=3
3. DOM with $N_\vartheta,N_\phi$=8

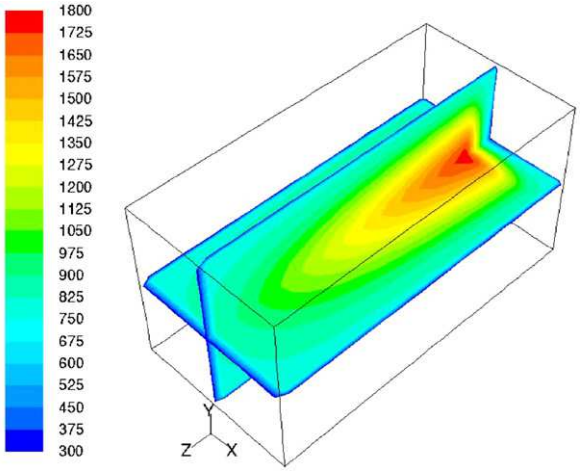


**Fig. 1.** Contours of temperature for Case 1 in K.

As shown in Fig. 2, results from all the methods of calculating RTE are in good agreement with the benchmark data. However the DOM method produces better agreement around the minimum in the radiative source term. The $P_1$ method is slightly less accurate in the prediction of the radiative source term in the region where the temperature gradient is steep. The $P_1$ method predictions are slightly less accurate than the DOM predictions due to the assumption of linear variation of radiation intensity with direction cosines and also the uncertainty in boundary condition [9]. Only the $N_\vartheta,N_\phi$=3 result is shown in Fig. 2 because the solution for $N_\vartheta,N_\phi$=8 was very similar and to avoid confusion they were omitted from this graph.

A comparison can also be made between the different methods for the absorption coefficient. In addition to the FSCK method, the best available model for calculating the properties of combustion gases in commercial CFD codes has been examined. This is the weighted sum of gray-gases method (WSGGM). In ANSYS FLUENT V12.0 CFD software, the correlations of Smith et al. [29] are used to calculate the total emissivity of a mixture of $CO_2$ and $H_2O$, then Beer's law is used to calculate a gray absorption coefficient based on the total emissivity and mean beam length of the chamber. The correlations computed by Smith et al. were for partial pressure ratios of water vapour to carbon dioxide of $[p_{H2O}/p_{CO2}]$=2 or $[p_{H2O}/p_{CO2}]$=1. These values are therefore only suitable for the products of air and gaseous fuel combustion. The implementation of the WSGGM in ANSYS FLUENT V12.0 is a gray method and is expected to be less accurate than the FSCK method. It is noted that the standard WSGGM is a non-gray method, but the implementation in CFD is gray to reduce the computation times, since it was used to calculate the total emissivity in order to obtain a gray absorption coefficient as discussed above.

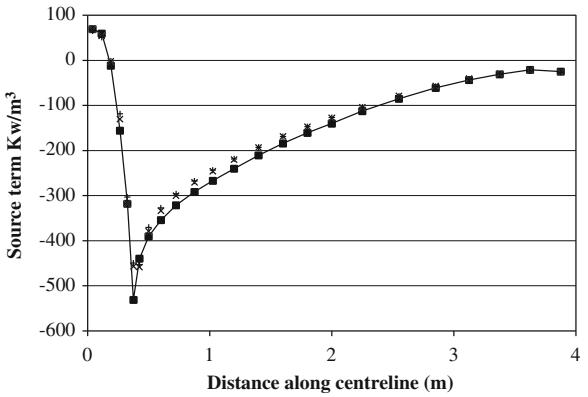


**Fig. 2.** Comparison of radiative source term along the centreline to benchmark data (■) using DOM $N_\vartheta,N_\varphi$=3 (×) and $P_1$ (+) methods with FSCK method for radiative properties (Case 1).

The standard calculation of the absorption coefficient using the WSGGM based on Smith's correlations can be compared to the FSCK model. For the WSGGM the mean pathlength of the enclosure was based on the law proposed by Hottel and Sarofim [30] evaluated based on the surface area ($A$) and volume ($V$) of the enclosure, MBL=3.6 V/A. Figs. 3 and 4 show results of the DOM coupled with both the FSCK and WSGGM. The quadrature used for both sets for results is $N_\vartheta,N_\phi=3$ because the solution indicates only a low sensitivity to increasing the quadrature to greater than three.

It can be seen from the results that using a non-gray method to calculate the radiative properties of the medium produces a much better agreement to the benchmark heat flux data than the gray case. The WSGGM with Smith's correlation with a gray formulation in CFD software over predicts the heat flux to the walls and gives a less accurate prediction of the radiative source term. Case 1 has the same value for the partial pressure ratio as the correlations developed to calculate the total emissivity using Smith's WSGGM model and therefore a large over-prediction of the heat fluxes was not anticipated, and highlights the errors that can be introduced when a gray gas is used for modelling gases with strong spectral variation in properties. In order to further examine the effect that a gray gas has on the radiative source term and heat flux calculations, another gray method was employed to model Case 1. The gray absorption coefficient was calculated using Planck's absorption coefficient [31]. A relationship between temperature and the Planck absorption coefficient has been tabulated by Sandia National Laboratory and was used to calculate the absorption coefficient. The results using this method were considerably less accurate when compared to the WSGGM and FSCK results see Fig. 5. The wall fluxes and radiative source terms were over predicted and it is recommended that this method for calculating the absorption coefficient should be treated with caution.

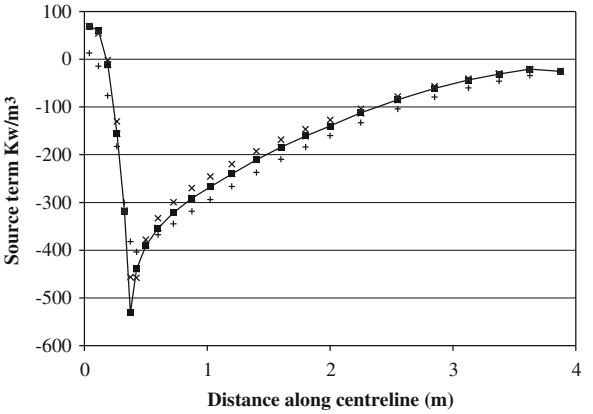


**Fig. 3.** Comparison of radiative source term of benchmark data (■) with DOM method using the non-gray FSCK (×) and gray WSSGM (+) for radiative properties (Case 1).

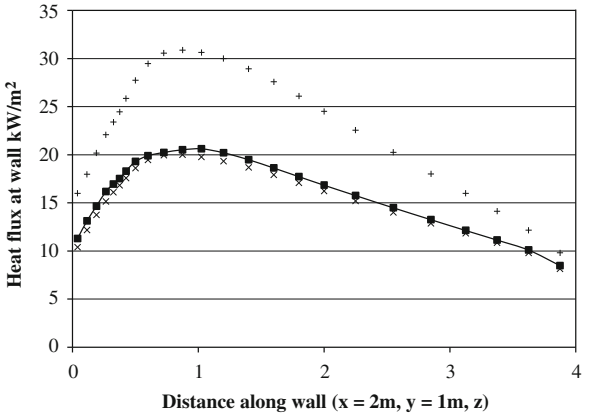


**Fig. 4.** Comparison of net radiative heat flux of benchmark data (■) with DOM with the non-gray FSCK (×) and gray WSSGM (+) for radiative properties (Case 1).

### 4.2. Case 2 (Air fired composition)

The second case considered for validation is similar to the Case 1 in terms of concentrations of the combustion gases and temperatures. The SNB benchmark data was published by Goutiere et al. [26] where it was compared to several other radiative property models including WSGGM (Smith's correlations with the non-gray implementation) and SLW. For the SNB data the RTE solver used is again a ray tracing method with $T_7$ quadrature. The enclosure modelled is a 2D rectangular enclosure with 1 m in the $x$ direction and 0.5 m in the $y$ direction. The concentrations of the combustion gases $CO_2$ and $H_2O$ are 10% and 20% by volume uniformly throughout the domain. The walls are kept at a cold temperature of 0 K. The temperature profile in the domain is given by two expressions, depending on the $x$ co-ordinate.

$$\text{for } x \le 0.1, T(x,y) = (14{,}000x - 400)(1 - 3y_0^2 + 2y_0^3) + 800$$

$$\text{for } x \ge 0.1, T(x,y) = \frac{-10{,}000}{9}(x-1)(1 - 3y_0^2 + 2y_0^3) + 800$$

where $y_0 = \frac{|y-0.25|}{0.25}$

The contours of temperature are shown in Fig. 6.

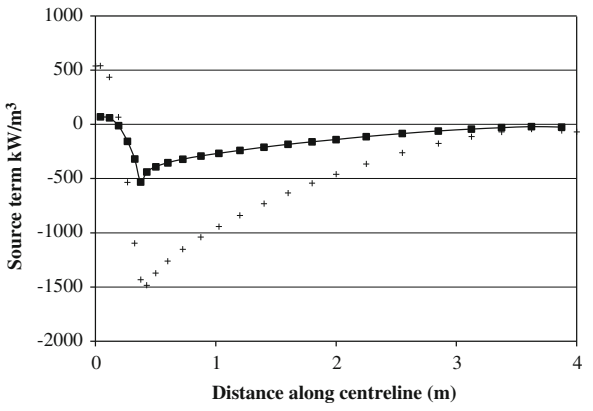


**Fig. 5.** Comparison of radiative source term of benchmark data (■) with DOM method using the gray Planck coefficient (+) for radiative properties (Case 1).

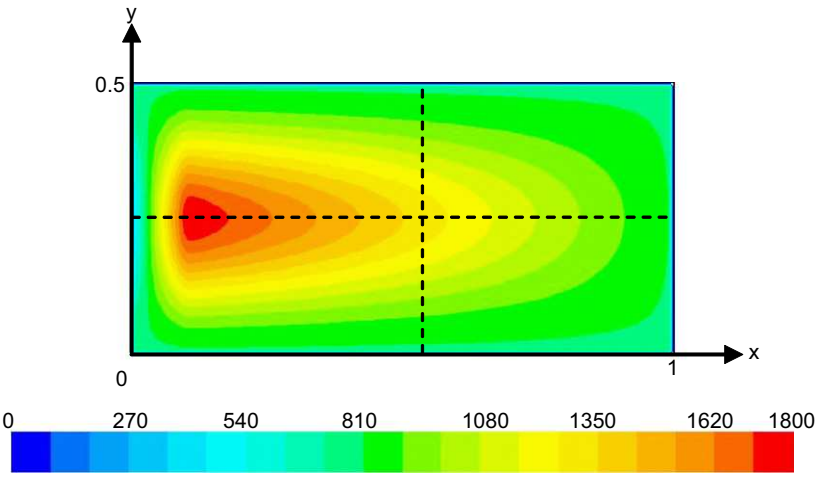


**Fig. 6.** Contours of temperature for Case 2 in K.

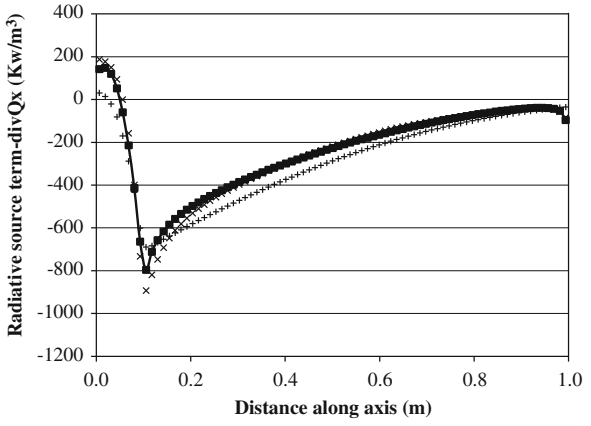


**Fig. 7.** Comparison of radiative source term along ($x$, 0.25) of benchmark data (■) with DOM method using the non-gray FSCK (×) and gray WSSGM (+) for radiative properties (Case 2).

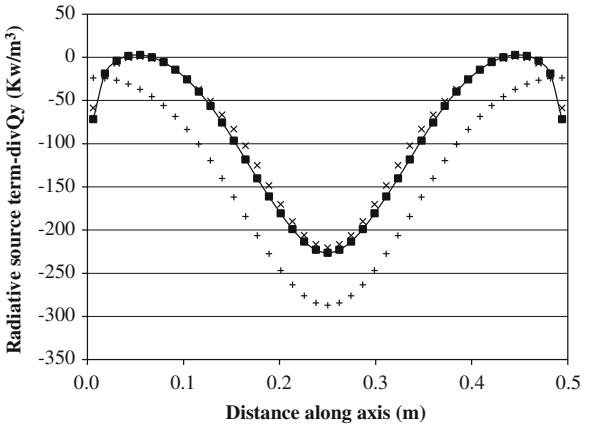


**Fig. 8.** Comparison of radiative source term along (0.5, $y$) of benchmark data (■) with DOM method using the non-gray FSCK (×) and gray WSSGM (+) for radiative properties (Case 2).

The data available for comparison to SNB data were again the radiative source term and net heat fluxes, in both the $x$ and $y$ directions. The dotted lines that intersect on Fig. 6 are the central lines in the $x$ and $y$ planes and indicate the locations for which the radiative source terms were compared. The top and right hand walls of the enclosure are used as the surfaces to compare the calculated heat fluxes. The grid used to calculate the DOM solution to Case 2 was chosen so that the nodes were in the same position as the grid used to calculate the SNB data. A finer discretization of the solid angle for the DOM was required to obtain accurate solutions so that $N_\vartheta$,$N_\phi$=8. Figs. 7 and 8 indicate the predicted source term along the centreline in the $x$ and $y$ directions. The DOM is used for the calculations for both the gray WSGGM and the FSCK calculations. A similar trend is observed in the agreement with the source terms along the $x$ direction, Fig. 7, as for Case 1. In particular the radiative source term along the $y$ direction, Fig. 8, is far better predicted with the FSCK than with the gray implementation of WSGGM.

The net radiative heat flux to the walls of the chamber is better predicted using the FSCK method than the WSGGM, although larger errors are observed with the heat flux in the $x$-direction, Fig. 9, than the $y$-direction, Fig. 10. The WSGGM over-predicts the net heat flux to the walls in both directions and the errors are substantial, up to 50%.

The results show that in general the FSCK method is superior when looking to match the predicted data to the SNB data, despite some errors being present. The differences between the FSCK and the SNB results can be at least partially attributed to the differences in the spectral data used. It is evident that the radiative source term (Fig. 7) is less well predicted around the minimum using the FSCK method in Case 2 than in Case 1 (Fig. 2).

### 4.3. Case 3 (Oxy-fired composition)

It has been shown the good agreement to the SNB data can be achieved using the FSCK method when the

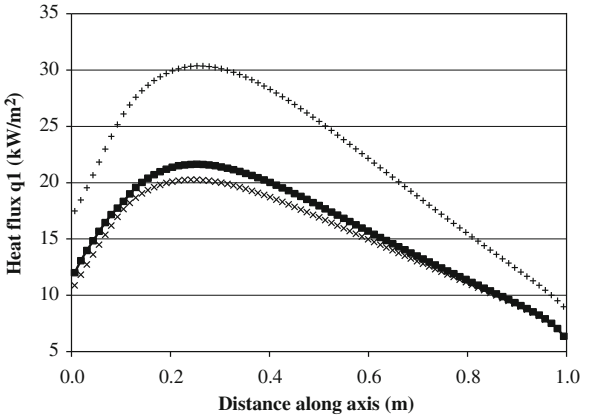


**Fig. 9.** Comparison of net radiative heat flux along ($x$, 0.5) of benchmark data (■) with DOM with the non-gray FSCK (×) and gray WSSGM (+) for radiative properties (Case 2).

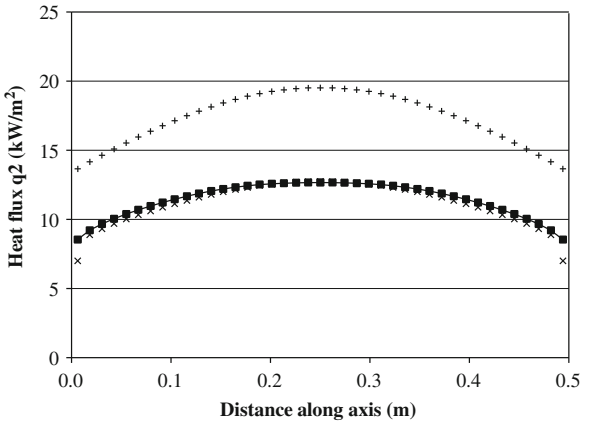


**Fig. 10.** Comparison of net radiative heat flux along (1, $y$) of benchmark data (■) with DOM with the non-gray FSCK (×) and gray WSSGM (+) for radiative properties (Case 2).

concentrations of $CO_2$ and $H_2O$ in the mixture are low. In order for the FSCK method to be viable for use in engineering CFD calculations for oxy-fuel combustion it must be proven to work at much higher concentrations of radiating species, especially $CO_2$, though theoretically the FSCK method can be applied at any concentration levels of $CO_2$ and $H_2O$. Therefore the same 3D geometry and temperature profile has been used as for Case 1 but with a composition of gases of 85% $CO_2$, 10% $H_2O$ and 5% $N_2$ by volume. These concentrations can be viewed as theoretical concentrations of oxy-fuel firing with dry RFG. The SNB data was computed as in Case 1 using a ray tracing method with $T_7$ quadrature and the DOM data was computed using $N_\vartheta$,$N_\phi$=4.

The partial pressure ratios for which the WSGGM correlations of Smith were developed are either $[p_{H2O}/p_{CO2}]$=2 or $[p_{H2O}/p_{CO2}]$=1. For Case 3 because of the very high $CO_2$ partial pressure the partial pressure ratio is $[p_{H2O}/p_{CO2}]$=0.1176 and hence is far outside the valid range for the use of Smith's correlations. The results

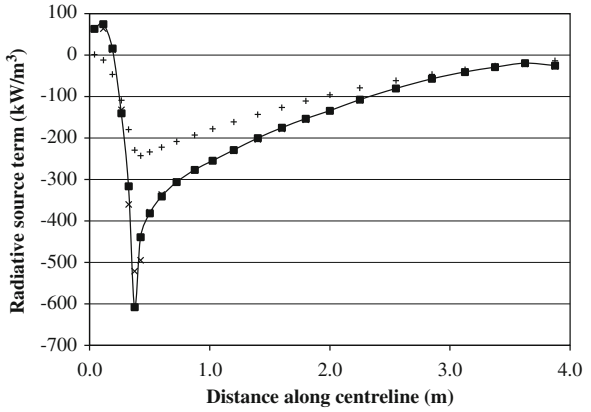


**Fig. 11.** Comparison of radiative source term along centreline of benchmark data (■) with DOM method using the non-gray FSCK (×) and gray WSSGM (+) for radiative properties (Case 3).

from this case enable the assessment of the WSGGM under oxy-fuel firing conditions. Fig. 11 indicates the errors introduced into the calculation of the radiative source term by using the WSGGM gray formulation for the radiative properties of high temperature gases representing oxy-fuel combustion products. The agreement between the benchmark SNB data and the DOM with FSCK is good for the radiative source term along the centreline. The WSGGM is under-predicting the source term significantly and this could lead to large errors in the prediction of the flame and environment temperature. The average error of the source term using FSCK is less than 5%, but using WSGGM the average error is greater than 50%.

A comparison can be made between the calculated incident radiation in the case with FSCK and WSGGM. Fig. 12 shows the calculated incident radiation for the two methods for Case 3. The peak in incident radiation is in the area of the highest temperature as expected, however the magnitude of the calculated incident radiation is much lower for the WSGGM case than with the FSCK method.

The net radiative heat flux at the walls of the enclosure from the FSCK method are in better agreement with the benchmark data than those from the WSGGM based on Smith's formulation. Fig. 13 shows the net flux on the end wall of the enclosure ($x$, $y$=1, $z$=4) and Fig. 14 shows the net heat flux on a side wall of the enclosure ($x$=0, $y$=1, $z$). The results from the FSCK method are in good agreement with the net radiative fluxes predicted by the SNB for both the end and the side walls, the WSGGM method does not predict the flux on the end wall correctly and although the trend of heat flux is predicted along the side wall, the actual values are lower especially at the end of the simulated furnace.

The prediction of the heat fluxes is substantially better for the WSGGM than the radiative source term. This highlights a cautionary note when considering using the standard WSGGM (with air-fired values) for oxy-fuel simulations. Because the radiative source term and incident radiation is under-predicted along with the

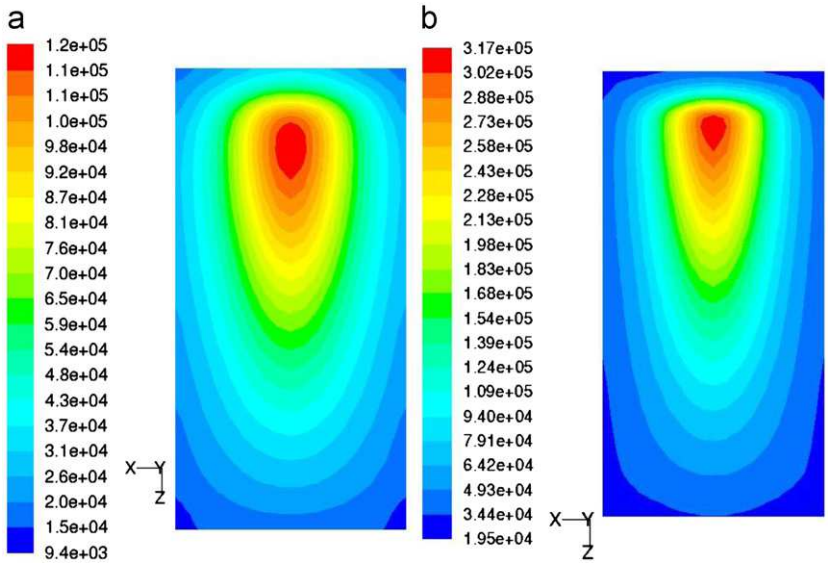


**Fig. 12.** Comparison of calculated incident radiation in central plane (w/m$^2$) (a) DOM with WSGGM and (b) DOM with FSCK (Case 3).

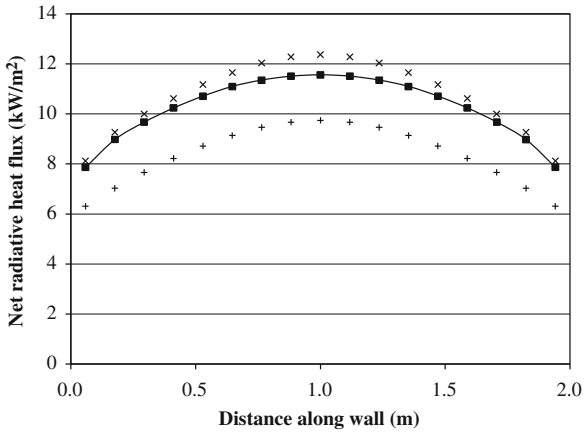


**Fig. 13.** Comparison of net radiative heat flux on $z$=4 m, $y$=1 m of benchmark data (■) with DOM with the non-gray FSCK ( × ) and gray WSSGM (+) for radiative properties (Case 3).

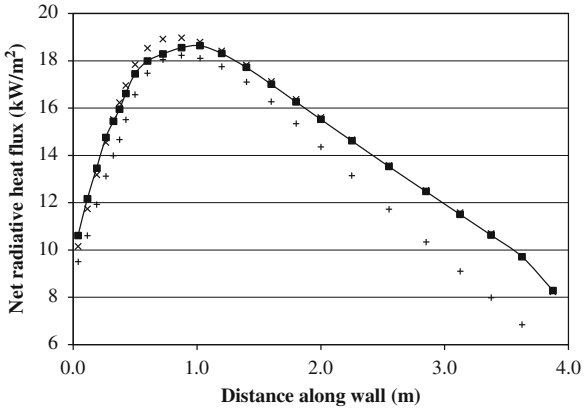


**Fig. 14.** Comparison of net radiative heat flux on $x$=1 m, $y$=1 m of benchmark data (■) with DOM with the non-gray FSCK ( × ) and gray WSSGM (+) for radiative properties (Case 3).

absorption coefficient, if the heat source (high temperature region) is close to the walls then the heat flux along the wall may appear to be correctly predicted because both of the contributing factors to how much radiation reaches the walls are under-predicted. However when the heat source is further from the walls as in the case with the end wall, the impact of the incorrect computation of the absorption coefficient and incident radiation is much more pronounced and leads to substantial errors.

When considering which RTE solver to use, one consideration is the optical thickness because the $P_1$ method should perform best at larger optical thicknesses. Hence the $P_1$ method should be expected to give better predictions in oxy-fuel combustion than for air combustion. To test this conjecture, the $P_1$ method was also used to compute the result for Case 3.

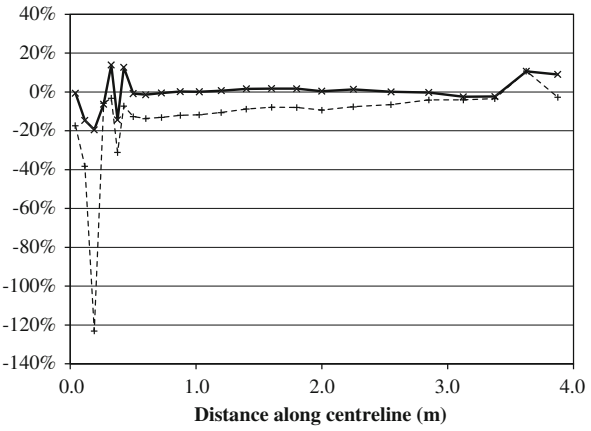


**Fig. 15.** Errors obtained when calculating the radiative source term using $P_1$ (+) and DOM ( × ) with FSCK method (Case 3).

**Table 1**
Comparison of CPU time per iteration.

| Method of RTE and absorption coefficient | $P_1$ and WSGGM | $P_1$ and FSCK | DOM and WSGGM ($N_\vartheta$,$N_\varphi$=4) | DOM and FSCK ($N_\vartheta$,$N_\varphi$=4/m) |
|---|---|---|---|---|
| **Ratio of CPU time** | 1 | 2.28 | 5.67 | 52.27 |

**Table 2**
Comparison of CPU time to reach a converged solution.

| Method of RTE and absorption coefficient | $P_1$ and WSGGM | $P_1$ and FSCK | DOM and WSGGM ($N_\vartheta$,$N_\varphi$=4) | DOM and FSCK ($N_\vartheta$,$N_\varphi$=4) |
|---|---|---|---|---|
| **Ratio of CPU time** | 1 | 298.95 | 5.59 | 76.16 |

Despite the higher optical thickness in Case 3 due to higher partial pressures of $CO_2$, the prediction of the radiative source term is less accurate when using the $P_1$ method than the DOM. The percentage error in the calculation of the source term is less than 20% for the DOM for all nodes, and for the majority the errors are close to 0%. However as Fig. 15 shows the errors using the $P_1$ approximation are much higher, especially near the regions of high temperature in the domain.

The different methods for solving the RTE and calculating the absorption coefficient require varying amounts of computational effort. The lowest calculation time is for the $P_1$ with the gray-WSGGM so all other methods CPU times are compared to this case. Table 1 shows the relative CPU times per iteration for the calculation of Case 3. It is evident that the $P_1$ method is substantially faster than the DOM per iteration, however the increase in computation time is dependent upon the quadrature that is chosen. Although the $P_1$ with FSCK solution is much faster per iteration than the DOM with FSCK, in reality the number of iterations required is much larger to reach convergence for the $P_1$ than DOM solution so it is also important to look at the computation time to reach a converged solution, as shown in Table 2. The $P_1$ solution in this case has not been optimised and a standard version has been used, with optimisation the number of iterations required may be reduced.

As the optical thickness of the case increases, from air firing to oxy-fuel firing, the computation time increased. However this was due to an increase in the quadrature of the DOM solution rather than the radiative properties model. Since the model calculates an absorption coefficient rather than a transmissivity, the optical thickness has less impact on the computational time of radiative properties than for some other methods.

## 5. Conclusions

Results of the FSCK method are in good agreement with the benchmark SNB data in all three test cases considered. The choice of absorption coefficient calculation on the results is most evident when a 'pseudo' oxy-fuel combustion system is considered with high partial pressures of $CO_2$. Using the standard gray-WSGGM case correlated with coefficients for fuel–air combustion can lead to substantial errors in the calculation of the radiative source term and hence greatly alters the predicted temperature distribution in the system in fully coupled calculations. Based on evidence from work presented in this paper, it is suggested that in order to improve the accuracy of temperature and heat transfer prediction in simulation of oxy-fuel combustion of gaseous or solid fuels, it is essential to use a non-gray spectral model such as the FSCK method. Significant errors are introduced when a gray method of computing the radiative properties is used and this is particularly evident when examining the heat fluxes to the walls of a system. The impact of using a gray or non-gray method is dependent on the case in question and is especially evident for oxy-fuel environments.

## Acknowledgements

The authors would like to thank EPSRC and Doosan Babcock Energy Limited for funding of this research. The authors would also like to thank Prof. Michael Modest and Dr. Anquan Wang (Penn State University) for allowing the use of the narrow band database of *k*-distributions and for continued help and discussion of this work.

## References

[1] Wall T, Liu Y, Spero C, Elliott L, Khare S, Rathnam R, et al. An overview on oxyfuel coal combustion—state of the art research and technology development. Chem Eng Res Des 2009;87:1003–16.
[2] Viskanta R, Menguc MP. Radiation heat transfer in combustion systems. Prog Energy Combust Sci 1987;13:97–160.
[3] Cheng P. Two-dimensional radiating gas flow by a moment method. AIAA J 1964:2.
[4] Sazhin SS, Sazhina EM, Faltsi-Saravelou O, Wild P. The P-1 model for thermal radiation transfer: advantages and limitations. Fuel 1996;75:289–94.
[5] Selcuk N, Kayakol N. Evaluation of discrete ordinates method for radiative transfer in rectangular furnaces. Int J Heat Mass Transfer 1997;40:213–22.
[6] Fiveland WA. Discrete-ordinates solutions of the radiative transport-equation for rectangular enclosures. ASME J Heat Transfer 1984;106:699–706.
[7] Lockwood FC, Shah NG. A new radiation solution method for incorporation in general combustion prediction procedures. Symp (Int) Combust 1981;18:1405–14.
[8] Modest MF. In: Radiative heat transfer. Academic Press; 2003.

[9] Liu F, Swithenbank J, Garbett ES. The boundary condition of the PN-approximation used to solve the radiative transfer equation. Int J Heat Mass Transfer 1992;35(8):2043–52.
[10] Chai JC, Lee HS, Patankar SV. Ray effects and false scattering in the discrete ordinates method. Numer Heat Transfer Part B 1993;24: 373–89.
[11] Saito M, Sadakata M, Sato M, Sakai T. Measurement of the temperature of burning, pulverized coal, using a high-speed, two-color pyrometer. Int Chem Eng 1989;29(3):494–502.
[12] Godoy SM, Lockwood FC. Development of a two-colour infrared pyrometer for coal particle temperature measurements during devolatalisation. Fuel 1997;77:995–9.
[13] Goody RMA. Statistical model for water-vapour absorption. Q J R Meteorol Soc 1952;78:165–9.
[14] Edwards DK, Balakrishnan A. Thermal radiation by combustion gases. Int J Heat Mass Transfer 1973;16:25–40.
[15] Liu F, Smallwood GJ. An efficient approach for the implementation of the SNB based correlated-k method and its evaluation. J Quant Spectrosc Radiat Transfer 2004;84:465–75.
[16] Modest MF. Narrow-band and full-spectrum k-distributions for radiative heat transfer-correlated-k vs. scaling approximation. J Quant Spectrosc Radiat Transfer 2003;76:69–83.
[17] Liu F, Guo H, Smallwood GJ. Effects of radiation model on the modeling of a laminar coflow methane/air diffusion flame. Combust Flame 2004;138:136–54.
[18] Ströhle J. Assessment of the re-ordered wide band model for non-grey radiative transfer calculations in 3D enclosures. J Quant Spectrosc Radiat Transfer 2008;109:1622–40.
[19] Denison MK, Webb BW. The spectral-line weighted-sum-of-gray-gases model for $H_2O/CO_2$ mixtures. ASME J Heat Transfer 1995;117:788–92.
[20] Solovjov VP, Webb BW. SLW modeling of radiative transfer in multicomponent gas mixtures. J Quant Spectrosc Radiat Transfer 2000;65:655–72.
[21] Modest MF, Zhang HM. The full-spectrum correlated-k distribution for thermal radiation from molecular gas–particulate mixtures. ASME J Heat Transfer 2002;124:30–8.
[22] Pierrot L, Soufiani A, Taine J. Accuracy of narrow-band and global models for radiative transfer in $H_2O$, $CO_2$, and $H_2O$–$CO_2$ mixtures at high temperature. J Quant Spectrosc Radiat Transfer 1999;62:523–48.
[23] Solovjov VP, Webb BW. The SLW Model: exact limits and relationships to other global methods. In: 2009 ASME Summer Heat Transfer Conference, San Francisco, USA, 2009.
[24] Modest MF, Riazzi RJ. Assembly of full-spectrum k-distributions from a narrow-band database; effects of mixing gases, gases and nongray absorbing particles, and mixtures with nongray scatterers in nongray enclosures. J Quant Spectrosc Radiat Transfer 2005;90:169–89.
[25] Wang A, Modest MF. High-accuracy, compact database of narrow-band k-distributions for water vapor and carbon dioxide. J Quant Spectrosc Radiat Transfer 2005;93:245–61.
[26] Goutiere V, Liu F, Charette A. An assessment of real-gas modelling in 2D enclosures. J Quant Spectrosc Radiat Transfer 2000;64: 299–326.
[27] Soufiani A, Taine J. High temperature gas radiative property parameters of statistical narrow-band model for $H_2O$, $CO_2$ and CO, and correlated-K model for $H_2O$ and $CO_2$. Int J Heat Mass Transfer 1997;40(4):987–91.
[28] Liu F. Numerical solutions of three-dimensional non-grey gas radiative transfer using the statistical narrow-band model. ASME J Heat Transfer 1999;121:200–3.
[29] Smith TF, Shen ZF, Friedman JN. Evaluation of coefficients for the weighted sum of gray gases model. ASME J Heat Transfer 1982;104: 602–8.
[30] Hottel HC, Sarofim AF. In: Radiative transfer. McGraw-Hill; 1967.
[31] International workshops on measurement and computation of turbulent nonpremixed flames. Sandia National Lab available at ⟨http://www.sandia.gov/TNF/radiation.html⟩; 2009.